

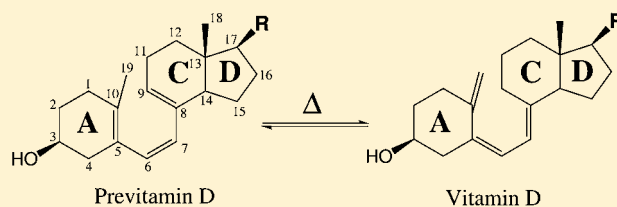
Tunneling and Conformational Flexibility Play Critical Roles in the Isomerization Mechanism of Vitamin D

Rubén Meana-Pañeda and Antonio Fernández-Ramos*

Department of Physical Chemistry and Centro Singular de Investigación en Química Biolóxica e Materiales Moleculares (CIQUS), Faculty of Chemistry, University of Santiago de Compostela, 15782 Santiago de Compostela, Spain

S Supporting Information

ABSTRACT: The thermal isomerization reaction converting previtamin D to vitamin D is an intramolecular [1,7]-sigmatropic hydrogen shift with antarafacial stereochemistry. We have studied the dynamics of this reaction by means of the variational transition-state theory with multidimensional corrections for tunneling in both gas-phase and *n*-hexane environments. Two issues that may have important effects on the dynamics were analyzed in depth, i.e., the conformations of previtamin D and the quantum effects associated with the hydrogen-transfer reaction. Of the large number of conformers of previtamin D that were located, there are 16 that have the right disposition to react. The transition-state structures associated with these reaction paths are very close in energy, so all of them should be taken into account for an accurate calculation of both the thermal rate constants and the kinetic isotope effects. This issue is particularly important because the contribution of each of the reaction paths to the total thermal rate constant is quite sensitive to the environment. The dynamics results confirm that tunneling plays an important role and that model systems that were considered previously to study the hydrogen shift reaction cannot mimic the complexity introduced by the flexibility of the rings of previtamin D. Finally, the characterization of the conformers of both previtamin D and vitamin D allowed the calculation of the thermal equilibrium constants of the isomerization process.



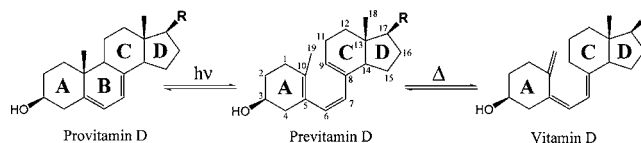
INTRODUCTION

Vitamin D is found in phytoplankton, which is one of the oldest forms of life. These organisms convert ergosterol (also called provitamin D₂) to previtamin D₂ when exposed to sunlight. After that previtamin D₂ isomerizes to vitamin D₂.^{1,2} It seems that ergosterol helps to protect the organism from ultraviolet (UV) radiation, which can be harmful for the genetic code. From these early forms of life, vitamin D₂ passed to fish and from there, through the food chain to more evolved organisms, preserving most of its character. Of the two known forms of vitamin D, for most mammals, including humans, the more active form is vitamin D₃, which differs from vitamin D₂ in the side chain of the sterol.

A deficiency of vitamin D leads to rickets, a common disease that afflicted children during the 19th and the beginning of the 20th centuries. The first studies on the subject pointed out the importance of taking cod-liver oil to prevent rickets,³ but in the 1920s scientists realized that sunlight was essential for the production of vitamin D₃ by the body^{4,5} and that vitamin D₃ promotes calcium deposition in the bones.⁶ Vitamin D₃ is produced from 7-dehydrocholesterol, a sterol that is present in the skin of most higher animals, so vitamin D₃ is not really a vitamin; i.e., it is a substance that the body can manufacture, and, therefore, its intake is not essential in the diet.^{7–9} Production of the two forms of vitamin D follows the same mechanism; i.e., the sterol or provitamin D, which is already present in the organism, is transformed by the action of UV radiation into previtamin D (Pre), which in turn thermally

isomerizes to vitamin D (Vit), the thermodynamically more stable of the two forms (see Scheme 1).

Scheme 1



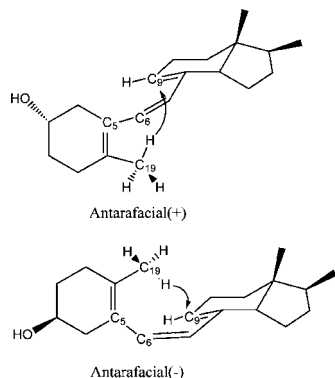
The UV light affects not only the first step of the reaction but also the thermal isomerization to Vit, because some side reactions are possible, e.g., closure of the B ring leading to lumisterol or rotation about the C₆–C₇ double bond (from *Z* to *E*) producing tachysterol. The production of these side products is reversible, due to the conformational flexibility of Pre.^{10,11} Thermal isomerization of Vit occurs by a [1,7]-sigmatropic hydrogen shift¹² when the C₅–C₆ and C₇–C₈ single bonds have *s-cis* conformations (*cZc*). From the experimental point of view it is not known which is the most stable form of Pre,¹³ although the theoretical calculations point to the *s-trans,s-cis* conformer (*tZc*) as the one with the lowest energy.^{14,15} The conformational analysis is complicated further by the flexibility of the A and C rings.

Received: August 15, 2011

Published: November 27, 2011

The thermal isomerization occurs with antarafacial stereochemistry.^{16–18} However, there are two possibilities for antarafacial hydrogen exchange: the *cis*-10,6,8-triene can twist in a right-handed sense, i.e., the dihedral angle about the bond C₅–C₆ is positive (the A ring is below the C ring), so we call this configuration antarafacial(+), or it can be antarafacial(–), i.e., the triene twists in a left-handed sense (the dihedral angle about the bond C₅–C₆ is negative), as shown in Scheme 2.

Scheme 2



Sheves et al.¹⁹ using ²H NMR and mass spectrometry techniques obtained that the hydrogen shift prefers a right-handed disposition by a ratio of 2:1. Those authors also reported a kinetic isotope effect (KIE) for the isomerization in isoctane of about 45 at 80 °C. A more reliable value of the KIE was measured by Okamura et al.²⁰ using a pentadeuterio derivative of Pre in *n*-hexane, and at the same temperature of reaction they obtained a KIE of 6.2. Baldwin and Reddy²¹ reported a KIE of 7.0 for the 7-methylocta-1,3(*Z*),5(*Z*)-triene (see Scheme 3) at 60 °C (hereafter, we refer to this triene

Scheme 3



simply as Tri); this KIE is very close to the value of 7.4 in Pre. The absolute values of the thermal rate constants are also close: 5.6×10^{-5} and $9.7 \times 10^{-5} \text{ s}^{-1}$ for Tri and Pre, respectively. The similarity in the experimental data indicates that Tri could be a good theoretical model to study the isomerization reaction.^{22,23}

Transition-state theory²⁴ on Tri at 60 °C led to a KIE of 3.9, which is almost half the experimental value. TST ignores quantum effects, but since the [1,7]-hydrogen shift is a hydrogen-transfer reaction,²⁵ Hess²² indicated that the discrepancy between the two KIEs may be due to quantum mechanical tunneling. In this context theoretical calculations based on variational transition-state theory with multidimensional tunneling corrections²⁶ (VTST/MT) can be of great help, because this theory incorporates quantum effects using semiclassical methods.^{27–29} The VTST/MT calculations on Tri²³ at 60 °C led to a KIE of 5.5, which is in much better agreement with the experimental value, and therefore there is strong evidence that tunneling plays an important role in [1,7]-hydrogen shift reactions. [Note: KIEs calculated using TST are usually called quasiclassical, because do not include quantum effects (with the exception of the zero-point energy effects). On

the other hand, KIEs calculated using VTST/MT are called semiclassical because quantum effects are incorporated semiclassically.]

The agreement between the experimental data of Tri and Pre may hide important differences, because both the KIEs and the thermal rate constants are cumulative properties that may be due to the contribution of several reacting structures. In Tri there are several equilibrium conformations, but only one has the right structure to react, whereas in Pre we expect to have many reactive configurations due to the flexibility of the rings. In other words, should we expect a strong influence of the A and C rings in the isomerization reaction? How is this flexibility going to affect the thermal rate constants and the tunneling effect?

The objective of this work is to analyze in detail, from a theoretical point of view, the dynamics of the isomerization reaction of Pre to answer the above questions. The rings bring complexity to the problem, and, therefore, their incorporation is crucial for the understanding of the isomerization reaction. This is a difficult task due to the large size of the molecule, especially if the goal is to obtain accurate thermal rate constants and, thus, accurate KIEs. It can be achieved by interfacing electronic structure calculations and VTST/MT. The latter has proved to be a powerful tool for getting insight into reaction mechanisms of complex systems,³⁰ and the present work is pioneering the use of this approach to study the isomerization reaction in the Pre.

On the other hand, the thermal rate constants for the isomerization reaction have also been measured in anisotropic environments such as human skin,³¹ liposomal models,³² and β -cyclodextrins,³³ the reactions being more than 10 times faster than in *n*-hexane. Tian et al.³¹ pointed out that a possible reason is that in human skin the amphipathic environment of the phospholipids would involve a larger participation of the antarafacial(–) attack.

To take into account the effect of the environment, we make a comparison of the gas-phase calculations with those obtained in *n*-hexane. The latter calculations also allow us to make a direct comparison with experiment.²⁰ The study of the isomerization reaction in anisotropic environments, for instance human skin, is out of the scope of this work. Still, we hypothesize about the mechanism of the process in these environments taking into account the previous experimental data and the results obtained in this work.

■ CALCULATION METHOD

The lateral chain (R in Scheme 1) distinguishes the two forms of Pre (i.e., D₂ and D₃). It plays a major role in the transformation of Vit into a hormone, but at this stage of the process, in both gas-phase and *n*-hexane environments, the lateral chain can be safely replaced by a methyl group, although we still preserve the names Pre and Vit to refer to these modified compounds.

All stationary-point geometries (equilibrium configurations and transition-state structures) were optimized by the MPWB1K density functional method³⁴ with the 6-31+G(d,p) basis set.³⁵ This level of theory was already used in the study of the [1,7]-hydrogen shift in Tri with very good results²³ and has shown to be adequate for nonmetallic thermochemical kinetics and thermochemistry.³⁶

Experimental measurements on the isomerization reaction of Pre were carried out in *n*-hexane,²⁰ so in order to take into account the effect of the solvent, we have performed SMS.43R continuum solvation model³⁷ single-point calculations on the gas-phase MPWB1K/6-31+G(d,p) geometries at the MPWB1K/6-31+G(d,p) level.³⁸ This solvation model has been extensively tested against experimental free energies of solvation for aqueous and organic

Table 1. Relative Values with Respect to the Pre_a(HC,HC)(+)tZ(-)c Conformer of Classical Energies (ΔE), Classical Energies Including Zero-Point Energy ($\Delta E(\text{ZPE})$), and Standard-State Free Energies at 37 °C in the Gas Phase (ΔG_g^X) and in *n*-Hexane (ΔG_s^X)^a

reaction	conformer	ΔE	$\Delta E(\text{ZPE})$	$\Delta G_g^X (T = 37 \text{ }^\circ\text{C})$	$\Delta G_s^X (T = 37 \text{ }^\circ\text{C})$
R1	Pre _{a(+)} (HC,HC)	1.50	1.44	0.72	0.63
	TS _{a(+)} (HC,HC)	27.97	25.42	26.38	26.46
	Vit _{a(+)} (CH,CH)	1.83	2.24	2.32	2.74
R2	Pre _{a(-)} (HC,HC)	1.48	1.83	1.86	2.07
	TS _{a(-)} (HC,HC)	29.61	27.32	28.25	28.38
	Vit _{a(-)} (T,CH)	5.91	6.38	6.70	7.15
R3	Pre _{a(+)} (HC,TB)	6.02	6.16	5.25	5.26
	TS _{a(+)} (HC,TB)	31.32	28.79	29.63	29.70
	Vit _{a(+)} (CH,T)	7.32	7.09	6.43	6.88
R4	Pre _{a(-)} (HC,TB)	5.61	6.07	5.90	6.04
	TS _{a(-)} (HC,TB)	29.63	27.30	28.36	28.46
	Vit _{a(-)} (T,T)	9.76	10.65	10.98	11.18
R5	Pre _{e(+)} (HC,HC)	1.73	1.92	1.80	1.77
	TS _{e(+)} (HC,HC)	28.35	25.48	26.31	26.21
	Vit _{e(+)} (T,CH)	7.83	7.70	7.16	7.65
R6	Pre _{e(-)} (HC,HC)	2.87	2.93	2.54	2.47
	TS _{e(-)} (HC,HC)	30.28	27.60	28.39	28.31
	Vit _{e(-)} (CH,CH)	2.57	2.81	3.07	3.61
R7	Pre _{e(+)} (HC,TB)	6.85	6.83	6.30	6.15
	TS _{e(+)} (HC,TB)	31.60	29.07	29.89	29.77
	Vit _{e(+)} (T,T)	13.41	13.21	12.01	12.43
R8	Pre _{e(-)} (HC,TB)	6.99	7.10	6.56	6.48
	TS _{e(-)} (HC,TB)	30.47	28.07	29.09	28.98
	Vit _{e(-)} (CH,T)	6.20	6.67	6.76	7.17
R9	Pre _{e(+)} (TB,HC)	6.64	6.37	5.14	5.20
	TS _{e(+)} (TB,HC)	29.60	27.15	28.05	28.11
	Vit _{e(+)} (T,CH)	7.22	7.59	7.29	7.71
R10	Pre _{e(-)} (TB,HC)	7.54	7.33	6.22	6.27
	TS _{e(-)} (TB,HC)	31.73	29.41	30.38	30.52
	Vit _{e(-)} (T,CH)	7.27	7.85	7.92	8.49
R11	Pre _{e(+)} (TB,TB)	11.42	10.52	7.73	7.92
	TS _{e(+)} (TB,TB)	33.10	30.39	30.85	30.89
	Vit _{e(+)} (T,T)	12.40	12.37	11.57	11.97
R12	Pre _{e(-)} (TB,TB)	11.61	11.72	10.68	10.68
	TS _{e(-)} (TB,TB)	32.02	29.32	29.98	30.09
	Vit _{e(-)} (T,T)	10.42	10.61	9.98	10.52
R13	Pre _{a(+)} (TB,HC)	–	–	–	–
	TS _{a(+)} (TB,HC)	28.60	26.22	27.22	27.30
	Vit _{a(+)} (T,CH)	5.77	5.85	1.02	1.25
R14	Pre _{a(-)} (TB,HC)	–	–	–	–
	TS _{a(-)} (TB,HC)	29.46	27.10	28.02	28.20
	Vit _{a(-)} (T,CH)	5.55	6.23	6.40	6.65
R15	Pre _{a(+)} (TB,TB)	11.02	11.12	10.05	9.76
	TS _{a(+)} (TB,TB)	31.99	29.26	29.79	29.81
	Vit _{a(+)} (T,T)	10.59	10.86	10.51	11.11
R16	Pre _{a(-)} (TB,TB)	10.01	10.03	8.93	9.08
	TS _{a(-)} (TB,TB)	29.72	27.03	28.00	28.17
	Vit _{a(-)} (T,T)	8.79	9.45	9.29	9.59

^aFor ΔG_g^X and ΔG_s^X , X = R (in Pre), ‡ (in TS), and P (in Vit). All values are in kcal/mol.

solvents with good results.^{37,39} The same type of calculations were carried out for the Tri system, so we could directly compare the [1,7]-hydrogen shifts in Pre and in Tri in this solvent.

In both gas-phase and *n*-hexane environments, all the VTST/MT calculations were performed using canonical variational transition-state theory (CVT),⁴⁰ and quantum effects were incorporated by the small-curvature tunneling (SCT) approach,⁴¹ so hereafter, we refer to this methodology as CVT/SCT. Thermal rate constants were also calculated by TST for comparison. These calculations were also

performed for the pentadeuterio derivative, Pre(*d*₅), isotopically substituted in the 9,14,19,19,19-positions, for which there are also experimental data available.²⁰

The total isomerization rate constant should take into account all the paths that lead to reaction, so it can be considered as a multipath (MP) rate constant. The rate constants of interconversion between conformers are much faster than the individual isomerization rate constants, so the multipath rate constant can be obtained using the generalized version⁴² of the Winstein–Holness equation⁴³ (see

Supporting Information). In this equation the multipath rate constant for isomerization using approximation Y (where $Y = \text{TST}$ or CVT/SCT) can be written as the weighted sum of the individual isomerization reactions, i.e.,

$$k^{\text{MP},Y}(T) = \sum_{i=1}^{n_R} W_i(T) k_i^Y(T) \quad (1)$$

where the weighting factor $W_i(T)$ is the statistical probability for the reaction occurring through path i , and n_R is the number of conformers that can lead to reaction. Computational details about the calculation of the CVT/SCT thermal rate constants, equilibrium constants, and kinetic isotope effects for the isomerization process can be found in the Supporting Information.

All the electronic structure calculations were performed with Gaussian03,⁴⁴ and the thermal rate constants were calculated with version 9.7 of the POLYRATE program.⁴⁵ The GAUSSRATE9.7⁴⁶ program linked the two packages. Free energies of solvation with the SM5.43R model were computed by a modified version of Gaussian03 called Minnesota Gaussian Solvation Model (MN-GSM), version 2009.⁴⁷

RESULTS AND DISCUSSION

There are several aspects of the thermal isomerization reaction of Pre that need careful consideration, so we have divided this section into several parts. First we discuss the most relevant conformational aspects of the stationary points of reaction (a complete description of the conformations is given in the Supporting Information). With this information about the conformers at hand it is straightforward to calculate the equilibrium constants. Finally we perform the dynamics calculations and obtain thermal rate constants and KIEs for the isomerization reaction in both the gas phase and *n*-hexane. The results are also compared with those obtained for the [1,7]-hydrogen shift reaction in Tri. The results on the statics and dynamics of the isomerization reaction were also used to get a hint about the same process in human skin and in other anisotropic environments.

Conformational Analysis. We have carried out an exhaustive conformational study of all the relevant stationary points (reactants, products, and transition-state structures) for the isomerization reaction. For the conformations of Pre we use the notation $\text{Pre}_p(\text{A,C})(\pm)qZ(\pm)r$, where p indicates the position of the OH group: pseudoaxial (a) or pseudoequatorial (e). The configurations [half-chair (HC) or twist-boat (TB)] of the A and C cyclohexene rings are indicated in parentheses. The letters q and r indicate the *s*-cis and *s*-trans disposition of the dihedral angles about the $\text{C}_5\text{--C}_6$ and $\text{C}_7\text{--C}_8$ single bonds, respectively, i.e., *s*-cis (\pm)c for dihedral angles between 0° and $\pm 90^\circ$, and (\pm)t for dihedral angles between $\pm 91^\circ$ and $\pm 180^\circ$. In Pre the $\text{C}_6\text{--C}_7$ double bond is always in *Z* configuration and the dihedral angle about the $\text{C}_7\text{--C}_8$ can only be (\pm)c due to steric impediments. Therefore, there are eight different conformations of the rings resulting from the combination of four conformations of the A ring with two conformations of the C ring. For each of the configurations of the rings, with the exception of $\text{Pre}_{a(\pm)}(\text{TB,HC})$ for which we could not locate any equilibrium structure, we have found five conformations by rotation about the single bonds. Of the five conformations, (+)cZ(+c) and (−)cZ(−)c are the equilibrium conformations for the antarafacial(+) and the antarafacial(−) [1,7]-hydrogen shifts, respectively. [Note: The notation for the reactive configurations can be abridged; for instance, the conformation $\text{Pre}_a(\text{HC,TB})(+)cZ(+c)$ can be shortened to $\text{Pre}_{a(+)}(\text{HC,TB})$. Hereafter we use the latter when referring to reactive

configurations.] Therefore, we have found 35 conformations, of which 14 are reactive. In the case of Vit, in parentheses are indicated the configurations [chair (CH) or twisted (T)] of the A and C cyclohexane rings. The $\text{C}_5\text{--C}_6$ and $\text{C}_7\text{--C}_8$ double bonds are in *Z* and *E* configurations, respectively, whereas the $\text{C}_6\text{--C}_7$ single bond is labeled as (\pm)c or (\pm)t as for the Pre single bonds. For the 16 transition-state structures we use the same notation as for Pre, although the conformation of the rings would be intermediate between Pre and Vit. [Note: Although we could not locate the $\text{Pre}_{a(\pm)}(\text{TB,HC})$ reactive structures, we could locate the $\text{TS}_{a(\pm)}(\text{TB,HC})$ transition-state structures.] Table 1 lists the energetics of the stationary points for each of the 16 reaction paths.

The relative stability of the equilibrium conformations is a result of the differences in energy between the conformations of the rings. Previous ab initio calculations indicated that HC is more stable than TB by about 5.5 kcal/mol in free cyclohexene,⁴⁸ and that CH is 4.3 kcal/mol more stable than T in 1,2-dimethylenecyclohexane.⁴⁹ Thus the Pre(HC,HC) and Vit(CH,CH) configurations are roughly ~8–12 kcal/mol more stable than the Pre(TB,TB) and Vit(T,T) configurations and ~4–6 kcal/mol more stable than the Pre(HC,TB), Pre(TB,HC), Vit(T,CH), and Vit(CH,T) configurations. The differences in energy due to conformational changes are smaller in the transition-state structures than in the equilibrium configurations, and they are mainly related to the disposition of the C ring. The antarafacial(+) attack is favored by the HC C-ring conformation of Pre, whereas the antarafacial(−) is favored by the TB C-ring conformation of Pre, and the final configuration of the C ring in Vit is of great importance in the stability of the transition states.

Thermodynamics Equilibrium Constants. Table 2 lists the calculated and experimental^{20,31} equilibrium constants for

Table 2. Calculated (Both in the Gas Phase, $K_{\text{eq,g}}$, and in *n*-Hexane, $K_{\text{eq,s}}$) and Experimental (K_{exp}) Equilibrium Constants for the Root Species, $\text{Pre}(d_0)$, and for the Pentadeuterated Compound, $\text{Pre}(d_5)$

T (°C)	$K_{\text{eq,g}}$	$K_{\text{eq,s}}$	K_{exp}^a
Pre(d_0)			
37.0	7.14	4.48	6.14, ^b 6.22 ^c
60.0	5.42	3.49	4.12 ^b
60.1	5.42	3.49	5.37 ± 0.41
69.35	4.89	3.19	4.53 ± 0.35
74.35	4.64	3.04	4.17 ± 0.32
79.9	4.38	2.88	3.82 ± 0.28
85.5	4.13	2.74	3.51 ± 0.25
Pre(d_5)			
60.5	6.12	3.98	5.42 ± 0.17
69.7	5.54	3.64	4.66 ± 0.19
74.1	5.29	3.49	4.36 ± 0.23
80.4	4.96	3.29	3.99 ± 0.25
85.5	4.72	3.15	3.72 ± 0.28

^aFrom ref 20 if not indicated otherwise. ^bFrom ref 31. ^cFrom ref 33.

the isomerization of the root species $\text{Pre}(d_0)$ and of the pentadeuterio derivative $\text{Pre}(d_5)$. The experimental equilibrium constants have been measured in *n*-hexane, and comparison with the calculated values in the same solvent shows that the stability of the Vit conformers is underestimated, although the calculations correctly predict the exoergodicity of the isomerization reaction. The equilibrium constants are completely

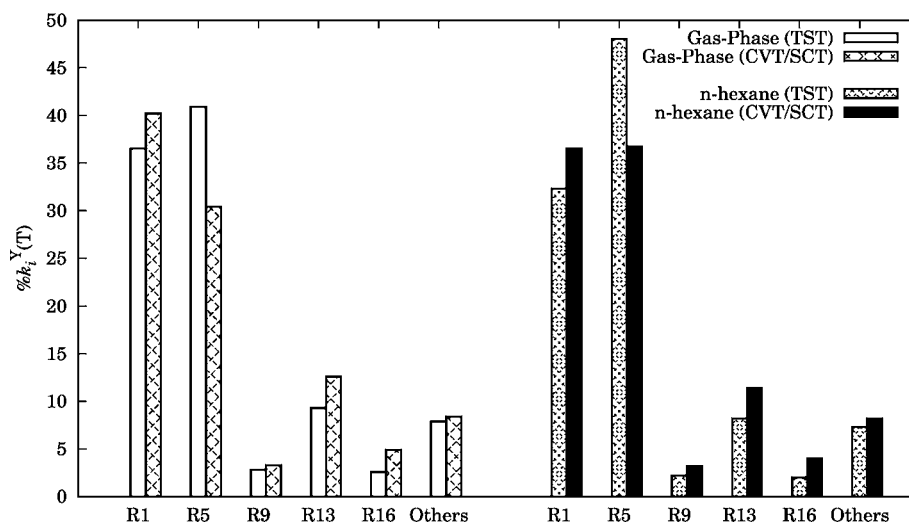


Figure 1. Histogram plotting the contributions of each of the individual reaction paths ($Y = \text{TST}$ or CVT/SCT) to the total rate constant in both the gas phase and *n*-hexane solution at $T = 37$ °C.

Table 3. Calculated and Experimental Thermal Rate Constants (in s^{-1}) for the [1,7]-Hydrogen and -Deuterium Shifts in Pre and Tri^a

Rate constant	Pre ($T = 37$ °C)		Pre ($T = 60$ °C)		Tri ($T = 60$ °C)	
	H	D	H	D	H	D
	Gas Phase					
$k^{\text{MP,TST}}$	1.18×10^{-6}	3.46×10^{-7}	1.87×10^{-5}	5.91×10^{-6}	1.02×10^{-5}	2.60×10^{-6}
$k^{\text{MP,CVT}}$	1.18×10^{-6}	3.42×10^{-7}	1.85×10^{-5}	5.84×10^{-6}	1.00×10^{-5}	2.60×10^{-6}
$k^{\text{MP,CVT/SCT}}$	1.27×10^{-5}	1.67×10^{-6}	1.39×10^{-4}	2.21×10^{-5}	4.80×10^{-5}	8.72×10^{-6}
	Solution					
$k^{\text{MP,TST}}$	9.09×10^{-7}	2.67×10^{-7}	1.44×10^{-5}	4.59×10^{-6}	1.10×10^{-5}	2.80×10^{-6}
$k^{\text{MP,CVT}}$	9.00×10^{-7}	2.64×10^{-7}	1.42×10^{-5}	4.54×10^{-6}	1.08×10^{-5}	2.80×10^{-6}
$k^{\text{MP,CVT/SCT}}$	9.00×10^{-6}	1.25×10^{-6}	1.01×10^{-4}	1.67×10^{-5}	5.17×10^{-5}	9.37×10^{-6}
k_{exp}	$6.8 \times 10^{-6}{}^b$	—	$9.72(\pm 0.03) \times 10^{-5}{}^c$	$1.32(\pm 0.034) \times 10^{-5}{}^c$	$5.6 \times 10^{-5}{}^d$	$8.0 \times 10^{-6}{}^d$
			$6.76 \times 10^{-5}{}^b$			

^aThe deuterated derivatives have been isotopically substituted in the 9,14,19,19-positions in Pre, and in the 7-position in Tri. ^bFrom ref 31. ^cFrom ref 20. The experimental temperatures are $T = 60.10(\pm 10)$ °C and $T = 60.50(\pm 10)$ °C for Pre(d_0) and Pre(d_5), respectively. The TST and CVT/SCT thermal rate constants listed in this table were calculated at the experimental temperatures. ^dFrom ref 21.

determined by the set of Pre(HC,HC) conformers and by the two (axial and equatorial) Vit(HC,HC)ZtE conformers. The differences between the calculated gas-phase and *n*-hexane solvent equilibrium constants show that there is a high sensitivity of the isomerization reaction to the environment.

The above calculations and the conformational study of the equilibrium configurations of both Pre and Vit may be useful to qualitatively describe the magnitude of the equilibrium constants obtained by Holick and co-workers^{31,33} in different anisotropic media. Those authors observed that at 37 °C the equilibrium constant varies from 1.76 in β -cyclodextrins to 11.44 in human skin. The large value of the equilibrium constant in human skin is similar to that obtained in liposomal models.³² Holick and co-workers³¹ pointed out that in the lipids there would be interactions that stabilize the *c*Zc conformers more than the *t*Zc conformers. These interaction would be a result of the amphipathic (with both hydrophilic and hydrophobic parts) nature of both phospholipids and Pre. The OH group of Pre would form a hydrogen bond with the hydrophilic part of the lipid (the phosphoric acid), and the hydrophobic part of Pre would interact with the acyl chain of the lipid by intermolecular dispersion forces. However, to our understanding it is difficult to find a reason why these

interactions should favor the *c*Zc conformers over the *t*Zc ones, and why this additional stabilization of the *c*Zc form, if present, should increase the equilibrium constant. An easier explanation would be that the most stable conformers of Vit would be stabilized further by these amphipathic interactions. When the isomerization reaction takes place in the presence of β -cyclodextrins, the equilibrium constant is near unity. Cyclodextrins are a family of compounds made up of sugar molecules bound together in a ring, and in the case of β -cyclodextrins the diameter of the cavity is about 6.2 Å. The isomerization reaction takes place inside of a cavity formed by the complexation of two β -cyclodextrin molecules. This cavity may not be large enough to allow rotations about the C_5-C_6 (in the case of Pre) or the C_6-C_7 (in the case of Vit) single bonds. The disappearance of the *t*Zc conformers of Pre and the ZtE conformers of Vit would decrease the value of the equilibrium constant substantially.

These results show that the environment plays a very important role in the relative stabilities of the equilibrium structures of Pre and Vit, and that from the thermodynamics point of view the formation of Vit is not favored by solvation in nonpolar organic solvents as *n*-hexane.

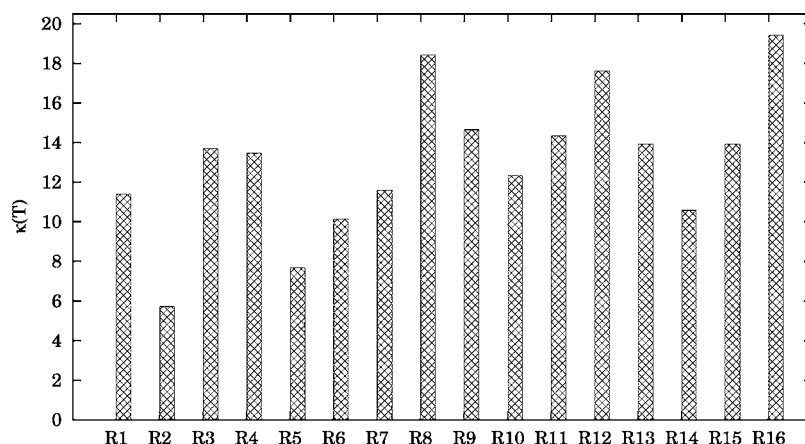


Figure 2. Histogram plotting the SCT transmission coefficients obtained in *n*-hexane for all the reactive channels at $T = 37$ °C.

Thermal Rate Constants. Calculation of the thermal rate constants was carried out at several temperatures in the interval between 25 and 95 °C, but here we limit the analysis of the thermal rate constants to mainly two temperatures: $T = 37$ °C (the normal body temperature) and $T = 60$ °C, one of the temperatures at which there are experimental results of thermal rate constants for the [1,7]-hydrogen shift reaction of both Tri and Pre. [Note: The experimental temperatures are $T = 60.0$ °C for Tri and $T = 60.10(\pm 10)$ °C for Pre, respectively. The thermal rate constants for Pre were calculated at $T = 60.1$ °C. However, in the text we use $T = 60$ °C and make a direct comparison between the Tri and Pre results.] The results at other temperatures can be found in the Supporting Information.

Figure 1 plots the contribution in percentage of each of the reaction paths at 37 °C, and Table 3 lists the total thermal rate constants for the isomerization reaction. The solvent has the effect of lowering the total CVT/SCT thermal rate constants by 30% due to changes in the free energy of activation (22%) and to the decrease in the tunneling transmission coefficients (8%). It also has an important effect on the two major reaction paths (R1 and R5), because the solvent favors the pseudoequatorial position of the OH group.⁵⁰ The rest of the channels increase the reactive flux by 26%. This percentage is not negligible, and it shows that is important to look for transition states coming from highly energetic (low populated) reactive conformers. The large number of reactive channels with low interconversion barriers between conformers may lead to situations in which there is hopping of reactive molecules between different channels. Variational transition-state theory cannot account for these nonstatistical effects, but to our understanding their impact on the thermal rate constants would be small. As an example, direct dynamics simulations carried out for the isomerization reaction in cyclohexane confirmed the presence of important nonstatistical effects.⁵¹ However, even in that case the TST thermal rate constants were in excellent agreement with the experimental data.

Quantum effects are of great importance for the isomerization reaction, because at 37 °C tunneling increases the thermal rate constants by an order of magnitude. Most of the tunneling occurs very close to the top of the barrier, and at 37 °C for reaction path R1, the tunneling energy that contributes the most to the transmission coefficient (sometimes called representative tunneling energy⁵²) is only 2.3 kcal/mol below the barrier. The SCT approximation describes well this type of

situation in which tunneling trajectories do not deviate substantially from the classical path for reaction, and it has been shown to perform well in other hydrogen shift reactions.⁵³ The SCT transmission coefficient for two major reaction paths diverge more than expected, i.e., 11.4 for R1 and 8.06 for R5, respectively (see Figure 2). This divergence can be traced to the difference in stability between the chair and twisted conformations of Vit, because the least stable product has a wider reaction path.

Figure 3 shows that the multipath CVT/SCT thermal rate constants are in very good agreement with the experimental

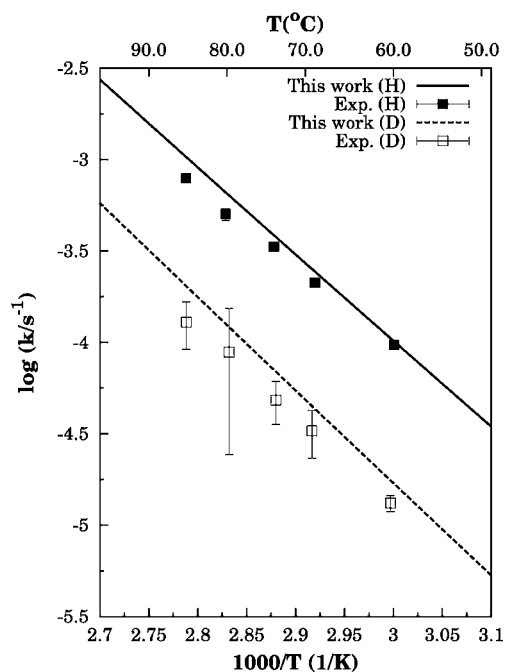


Figure 3. Arrhenius plot that compares experimental and multipath CVT/SCT thermal rate constants in *n*-hexane for both Pre(d_0) and Pre(d_5).

data from ref 20. In *n*-hexane the antarafacial(+) attack at $T = 80$ °C contributes about 86%. This value is in agreement with experimental measurements by Sheves et al.¹⁹ that showed that the antarafacial(+) attack is preferred, although our percentage is somewhat larger than the 67% predicted by those authors. Anisotropic microenvironments such as the skin

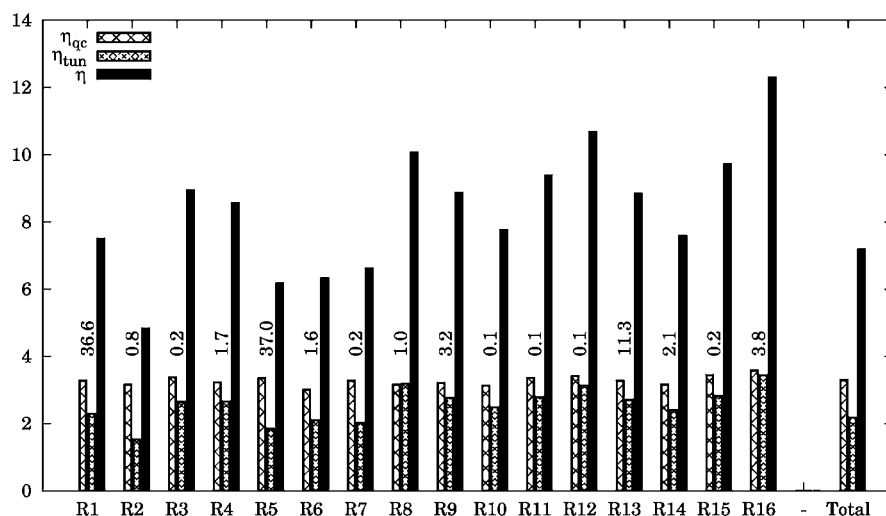


Figure 4. Histogram plotting the quasiclassical, η_{qc} , and quantum, η_{tun} , contributions of each of the isomerization reaction paths of Pre to the total KIE at $T = 37$ °C. The contribution in percentage, $\% \eta_p$, of each of the paths to the final KIE is indicated next to the bars. The resulting quasiclassical, quantum, and total KIEs are plotted in the last three bars.

may accommodate some of the conformers of Pre and their corresponding transition states better than isotropic environments (as *n*-hexane), because Pre itself has some anisotropy, with a hydrophilic hydroxyl group in the A ring when the rest of the molecule is hydrophobic. Stabilization of those highly energetic antarafacial(−) reactants with the C ring in the twisted-boat form would not modify the contribution of reactants to the final rate constants, since that is dominated by the half-chair conformations. However, it may involve a substantial increase of the contribution of the transition states. For instance, an additional stabilization of these reactants and transition states with respect to the antarafacial(+) stationary points by about 1.7 kcal/mol would increase the thermal rate constants by roughly a factor of 3.

That is not the only possibility for increasing the thermal rate constants, since it may also happen that, in this environment, the most stable conformations of Pre would be less stabilized than the transition states. This may also happen in β -cyclodextrins, which catalyze the isomerization reaction, making it almost 5 times faster than in human skin at 37 °C. In this case, as it was pointed out in the equilibrium constants section, we believe the disappearance of both the tZc conformers of Pre and the ZtE conformers of Vit due to steric hindrance aids the reaction even more. This would lead to lower values of the equilibrium constants, but to higher thermal rate constants than in human skin, because the most stable conformation of Pre would be cZc, which has a lower barrier for reaction than tZc.

The flexibility of the trienic system lowers the thermal rate constants for both Tri and Pre with respect to more rigid systems, because there is an expansion of the space of reactants. However, in Pre there is an additional flexibility due to the rings that leads to further expansion of the space of reactants but with an increase of reactivity that compensates it. Thus, at 60 °C the sum of the reactive flux of all channels makes the multipath thermal rate constant of Pre about 50% higher than the thermal rate constant of Tri. Another important difference between Pre and Tri is that for the latter the two possible antarafacial attacks lead always to transition states that are enantiomers; therefore, each of them contributes 50%. In Pre this percentage may fluctuate depending on the environment. Table 3 shows that the rate constants of Pre are more affected

by the environment than those of Tri, but, on the other hand, Tri would be much less efficient than Pre in anisotropic media. This is an indication that higher sensitivity to the environment is related to more flexibility.

Kinetic Isotope Effects. The KIEs of each of the reaction paths (in *n*-hexane) with their contribution to the total KIE are plotted in Figure 4 at 37 °C. The gas-phase KIEs (not plotted) are slightly larger than those in *n*-hexane, and the total KIE is about 6% larger in *n*-hexane, i.e., 7.62 versus 7.20. A comparison between Figures 2 and 4 shows that transmission coefficients and the KIEs change in the same fashion, because the quasiclassical contribution to the individual KIEs varies much more uniformly than the tunneling contribution. As indicated in the percentages of Figure 4, the two reaction paths that contribute the most to the final KIE are R1 and R5, and the individual KIEs are 7.49 and 6.40, respectively. The total KIE (7.20) is somewhat larger than the average of these two values (6.95) due to the contribution of the other reaction paths (mainly R13 and R16), which have larger tunneling contributions to the KIE than these two reaction paths. In general, environments like *n*-hexane, that stabilize reaction path R5, would lead to lower KIEs than environments that preferentially stabilize R1, R13, or R16. From these data we point out that a good low-limit for the total KIE for the isomerization reaction is the individual KIE of reaction R5.

At 60 °C the experimental KIEs are 7.4 and 7.0 for Pre and Tri, respectively, whereas the theoretical calculations in *n*-hexane are 6.01 and 5.52, respectively. The agreement between them is reasonable (the theoretical KIEs are lower by about 20%), taking into account the uncertainty in the experimental measurements, especially in the thermal rate constants for the deuterium transfer (see Figure 3), and the fact that we are using the harmonic-oscillator approximation, when there is some evidence that anharmonicity may have some influence on the value of the KIEs.⁵⁴

Even when both systems have quite similar total KIEs, the partial KIE contributions are quite different. The quasiclassical contribution is larger in Tri, but the tunneling contribution is larger in Pre. In this case, the quasiclassical contribution to the KIE would be mainly due to vibration, so this contribution would be more important when the difference between the free

energies of activation for the root and isotopically substituted species is large. As to the tunneling contribution to the KIE, it was expected to be larger for Pre than for Tri, because $\eta_{\text{tun}}(T)$ increases when the tunneling transmission coefficients are larger. This is consistent with a faster decay of the KIE for Pre than for Tri in the interval of temperatures between 25 and 95 °C.

Finally, we note that the R8, R12, and R16 reaction paths have large KIEs due to the tunneling contribution. Therefore, if in human skin the thermal rate constants are larger than in *n*-hexane due to an increase in the contribution of the antarafacial(−) attack, an experiment including measurements of the isotopically substituted Pre would display larger KIEs than those measured in *n*-hexane.

CONCLUDING REMARKS

We have carried out an exhaustive variational transition-state theory theoretical study using the CVT/SCT approach on the [1,7]-hydrogen shift reaction (or isomerization reaction) of Pre in both gas-phase and *n*-hexane environments. The conformational analysis of the equilibrium structures leads to a total of 35 conformers of Pre and 24 conformers of Vit.

The great flexibility of the A and C rings leads to 16 reaction paths for isomerization, and in both gas-phase and *n*-hexane environments the reaction occurs about 90% through antarafacial(+) attack. Although the contribution of the two of reaction paths obtained from the most stable configurations of Pre to the thermal rate constants and to the KIEs is substantial (about 74% at 37 °C), the contributions from some of the other reaction paths are relatively important and cannot be neglected. Therefore, the flexibility of the rings generates additional reactive flux. Additionally, these less important reaction paths increase the tunneling contribution as well as the KIE. The narrow energy window in which the transition states were located makes the hydrogen shift reaction quite sensitive to the environment, and we suggest that a further stabilization of some of the transition states may be the reason for the isomerization reaction to be faster in human skin (anisotropic environment) than in *n*-hexane (isotropic environment).

The comparison between Pre and Tri shows that, although the trienic system is identical for the two systems, their dynamics is quite different. Tunneling is more important in Pre than in Tri, and for the former, in both gas-phase and *n*-hexane environments, there is a preference for the antarafacial(+) attack—a preference that cannot exist in Tri.

ASSOCIATED CONTENT

Supporting Information

Section S.1, computational details on the CVT/SCT thermal rate constants, the equivalence between the generalized Winstein–Holness equation and eq 1, the equilibrium constants, and the KIEs; section S.2, geometries and energetic parameters of all the relevant stationary points for the isomerization reaction as well as a discussion about the relative stability of the transition states and some of the barriers for interconversion between conformers; sections S.3–S.6, data at several temperatures between 298 and 400 K in both gas-phase and *n*-hexane environments and for the Pre(d_0) and Pre(d_5) species (S.3, total TST, CVT, and CVT/SCT thermal rate constants; S.4, SCT transmission coefficients and the contribution of each of the individual reaction paths to the total TST, CVT, and CVT/SCT thermal rate constants; S.5, total KIEs; and S.6, contribution of each of the reaction paths

to the total KIEs); section S.7, thermal rate constants and KIEs of Tri in *n*-hexane; section S.8, complete refs 44 and 45. This material is available free of charge via the Internet at <http://pubs.acs.org>.

AUTHOR INFORMATION

Corresponding Author

qf.ramos@usc.es

ACKNOWLEDGMENTS

R.M.-P. and A.F.-R. thank Centro de Supercomputación de Galicia (CESGA) and the Minnesota Supercomputing Institute for computer time.

REFERENCES

- (1) Holick, M. F. In *Vetebrate Endocrinology: Fundamentals and Biomedical Implications*; Pang, P. K. T., Schreiber, M. P., Eds.; Academic Press: Orlando, FL, 1989; p 7.
- (2) Holick, M. F. *J. Cell. Biochem.* **2003**, *88*, 296.
- (3) Mellanby, E.; Cantag, M. D. *Lancet* **1919**, 196, 407.
- (4) Hess, A. F. *Am. J. Public Health* **1922**, *12*, 104.
- (5) Goldblatt, H.; Soames, K. N. *Biochem. J.* **1923**, *17*, 294.
- (6) McCollum, E. V.; Simmonds, N.; Becker, J. E.; Shipley, P. G. *J. Biol. Chem.* **1922**, *53*, 293.
- (7) Rosenfeld, L. *Clin. Chem.* **1997**, *43*, 680.
- (8) Holick, M. F.; Chen, T. C.; Lu, Z.; Sauter, E. *J. Bone Miner. Res.* **2007**, *22*, 28.
- (9) Deluca, H. F. In *Vitamin D*; Feldman, D., Pike, J. W., Glorieux, F. H., Eds.; Elsevier, Inc.: Amsterdam, The Netherlands, 2005; Vol. 1, p 3.
- (10) Jacobs, H. J. C.; Havinga, E. *Adv. Photochem.* **1979**, *11*, 305.
- (11) Holick, M. F. In *Vitamin D*; Feldman, D., Pike, J. W., Glorieux, F. H., Eds.; Elsevier, Inc.: Amsterdam, The Netherlands, 2005; Vol. 1, p 37.
- (12) Schlattmann, J. L. M. A.; Pot, J.; Havinga, E. *Recl. Trav. Chim. Pays-Bas* **1964**, *83*, 1173.
- (13) Dauben, W. G.; Funhoff, D. J. H. *J. Org. Chem.* **1988**, *53*, 5376.
- (14) Dauben, W. G.; Funhoff, D. J. H. *J. Org. Chem.* **1988**, *53*, 5370.
- (15) Dmitrenko, O.; Frederick, J. H.; Reischl, W. *J. Photochem. Photobiol. A* **2001**, *139*, 125.
- (16) Hess, B. A. Jr.; Schaad, L. J.; PanciX, J. *J. Am. Chem. Soc.* **1985**, *107*, 149.
- (17) Hoeger, C. A.; Okamura, W. H. *J. Am. Chem. Soc.* **1985**, *107*, 268.
- (18) Hoeger, C. A.; Johnston, A. D.; Okamura, W. H. *J. Am. Chem. Soc.* **1987**, *109*, 4690.
- (19) Sheves, M.; Berman, E.; Mazur, Y.; Zaretskii, Z. V. I. *J. Am. Chem. Soc.* **1979**, *101*, 1882.
- (20) Okamura, W. H.; Elnagar, H. Y.; Ruther, M.; Dobreff, S. *J. Org. Chem.* **1993**, *58*, 600.
- (21) Baldwin, J. E.; Reddy, P. *J. Am. Chem. Soc.* **1988**, *110*, 8223.
- (22) Hess, B. A. Jr. *J. Org. Chem.* **2001**, *66*, 5897.
- (23) Mousavipour, S. H.; Fernández-Ramos, A.; Meana-Pañeda, R.; Martínez-Núñez, E.; Vázquez, S.; Ríos, M. A. *J. Phys. Chem. A* **2007**, *111*, 719. **2011**, *115*, 9322.
- (24) Eyring, H. *J. Chem. Phys.* **1935**, *3*, 107.
- (25) *Hydrogen-Transfer Reactions*; Hynes, J. T., Schowen, R. L., Klinman, J. P., Limbach, H. H., Eds.; Wiley-VCH: Weinheim, 2007.
- (26) Fernández-Ramos, A.; Ellingson, A.; Garrett, B. C.; Truhlar, D. G. *Rev. Comput. Chem.* **2007**, *23*, 125.
- (27) (a) Hirschfelder, J. O.; Wigner, E. *J. Chem. Phys.* **1939**, *7*, 616. (b) Johnston, H. S. *Gas Phase Reaction Rate Theory*; Ronald Press: 1966. (c) Kuppermann, A. *J. Phys. Chem.* **1979**, *83*, 171.
- (28) Truhlar, D. G.; Kupperman, A. *J. Am. Chem. Soc.* **1971**, *93*, 1840.
- (29) Garrett, B. C.; Truhlar, D. G.; Grev, R. S.; Magnuson, A. W. *J. Phys. Chem.* **1980**, *84*, 1730.
- (30) Pu, J.; Gao, J.; Truhlar, D. G. *Chem. Rev.* **2006**, *106*, 3140.

- (31) Tian, X. Q.; Chen, T. C.; Matsuoka, L. Y.; Wortsman, J.; Holick, M. F. *J. Biol. Chem.* **1993**, *268*, 14888.
- (32) Tian, X. Q.; Holick, M. F. *J. Biol. Chem.* **1999**, *274*, 4174.
- (33) Tian, X. Q.; Holick, M. F. *J. Biol. Chem.* **1995**, *270*, 8706.
- (34) Zhao, Y.; Lynch, B. J.; Truhlar, D. G. *J. Phys. Chem. A* **2004**, *108*, 6908.
- (35) Hehre, W. J.; Ditchfield, R.; Pople, J. A. *J. Chem. Phys.* **1972**, *56*, 2257.
- (36) Zhao, Y.; Schultz, N. E.; Truhlar, D. G. *J. Chem. Theory Comput.* **2006**, *2*, 364.
- (37) Thompson, J. D.; Cramer, C. J.; Truhlar, D. G. *J. Phys. Chem. A* **2004**, *108*, 6532.
- (38) Lynch, B. J.; Fast, P. L.; Harris, M.; Truhlar, D. G. *J. Phys. Chem. A* **2000**, *104*, 4811.
- (39) Thompson, J. D.; Cramer, C. J.; Truhlar, D. G. *Theor. Chem. Acc.* **2005**, *113*, 107.
- (40) Garrett, B. C.; Truhlar, D. G. *J. Chem. Phys.* **1979**, *70*, 1593.
- (41) (a) Skodje, R. T.; Truhlar, D. G.; Garrett, B. C. *J. Phys. Chem.* **1981**, *85*, 3019. (b) Liu, Y.-P.; Lynch, G. C.; Truong, T. N.; Lu, D.-h.; Truhlar, D. G. *J. Am. Chem. Soc.* **1993**, *115*, 2408.
- (42) Baldwin, J. E.; Raghavan, A. S.; Hess, B. A. Jr.; Smentek, L. J. *Am. Chem. Soc.* **2006**, *128*, 14854.
- (43) Winstein, S.; Holness, N. J. *J. Am. Chem. Soc.* **1955**, *77*, 5562.
- (44) Frisch, M. J.; et al. *Gaussian03*; Gaussian, Inc.: Pittsburgh, PA, 2003.
- (45) Corchado, J. C.; et al. *POLYRATE*, version 9.7; University of Minnesota: Minneapolis, MN, 2007.
- (46) Corchado, J. C.; Chuang, Y.-Y.; Coitixio, E. L.; Ellingson, J.; Zheng, J.; Truhlar, D. G. *GAUSSRATE*, version 9.7; University of Minnesota: Minneapolis, MN, 2007.
- (47) Marenich, A. V.; Kelly, C. P.; Thompson, J. D.; Hawkins, G. D.; Chambers, C. C.; Giesen, D. J.; Winget, P.; Cramer, C. J.; Truhlar, D. G. *Minnesota Solvation Database*, version 2009; University of Minnesota: Minneapolis, MN, 2009.
- (48) Shishkina, S. V.; Shishkin, O. V.; Leszczynski, J. *Chem. Phys. Lett.* **2002**, *354*, 428.
- (49) Hofmann, H.-J.; Cimiraglia, R. *J. Org. Chem.* **1990**, *55*, 2151.
- (50) Lambert, J. B.; Marko, D. E. *J. Am. Chem. Soc.* **1985**, *107*, 7978.
- (51) Kakhiani, K.; Lourderaj, U.; Hu, W.; Birney, D.; Hase, W. L. *J. Phys. Chem. A* **2009**, *113*, 4570.
- (52) Kim, Y.; Truhlar, D. G.; Kreevoy, M. M. *J. Am. Chem. Soc.* **1991**, *113*, 7837.
- (53) Shelton, G. R.; Hrovat, D. A.; Borden, W. T. *J. Am. Chem. Soc.* **2007**, *129*, 164.
- (54) Wong, K. Y.; Richard, J. P.; Gao, J. *J. Am. Chem. Soc.* **2009**, *131*, 13963.